

# Morphological EMD Based Image Fusion Using Image Statistics

T.Yaswitha<sup>1\*</sup>, D.Anuradha<sup>2</sup>, K.Nikhil<sup>3</sup>, M.Sivareddy<sup>4</sup>, M.V.Srikanth<sup>5</sup>

<sup>[1],[2],[3],[4],[5]</sup> Department of ECE, Usha Rama College of Engineering and Technology

tellayaswitha@gmail.com, danduboyeenaanuradha@gmail.com, knikhilnikhil077@gmail.com, sivared  
dymuthikepalli@gmail.com, sree.02476@gmail.com

## ABSTRACT

*This work introduces a new and quick method for image fusion using morphological filters that is based on empirical mode decomposition (EMD). First, we create a multi-channel, bi-dimensional EMD technique for image fusion that is based on morphological filters. It can divide the input source images into many intrinsic mode functions (IMFs) with varying scales and a residue. It computes the upper and lower envelopes of a multi-channel image in the sifting processing using the morphological expansion and erosion filters. For multi-channel images, it considerably increases the calculation efficiency of EMD while preserving the decomposition quality. Second, rather than using the pixel-based fusion method typically employed in EMD-based image fusion, we employ a patch-based fusion strategy with overlapping partition to fuse the IMFs and residue. In this method, an image statistics-based weighted average rule is designed to fuse the IMFs, and the feature information extracted by IMFs is used as a guide to merge the residue. In addition to effectively extracting the significant information from the source images, this technique can lessen the spatial artifacts caused by the noisy pixel-wise maps. Numerous comparison tests on the fusing of multiple widely-used image data sets containing multi-focus and multi-modal images demonstrate that our recently suggested fusion method can get significantly better outcomes than the current EMD-based image fusion techniques. It also faces intense competition in terms of visualization, objective metrics, and time performance from the most advanced image fusion techniques.*

**Keywords:** morphological filter, empirical mode decomposition, intrinsic mode functions, image fusion, image statistics.

---

## 1. INTRODUCTION

With the rapid progress of data acquiring technology, a variety of sensors capturing images are emerging. Although each sensor has irreplaceable advantages in its appropriate working condition and range, the information obtained according a single imaging sensor is incomplete. Image fusion is an important technique to integrate image data of the same target collected by multi-sensors, so as to extract the favorable information in each sensor to the greatest extent and synthesize it into high-quality images. They are more suitable for human visual perception and further image processing tasks [1]. Image fusion has been extensively used in computer vision, military, remote sensing, etc. [2].

By adaptively breaking down a 1D time series signal into multiple intrinsic mode functions (IMFs) and a residue through iterative sifting processing, the classical empirical mode decomposition (EMD) developed by Huang et al. [3] is a potent tool for processing non-stationary and nonlinear one-dimensional signals. It may also adaptively represent the feature information with varied scales of input source images. This extension to 2D images is known as bi-dimensional empirical mode decomposition (BEMD). A lot of researchers have used EMD in image fusion to get beyond the problems caused by specified basis functions in fusion techniques that rely on traditional transforms like wavelet and Fourier transforms. Unfortunately, because there are still some issues that need to be resolved, the current EMD-based image fusion techniques [4–11] have little effect on picture fusion. First off, the envelope generation in the 2D picture sifting processing becomes extremely time-consuming as the image size rapidly increases, especially for the surface interpolation-based EMD methods. This makes the computation

efficiency of such approaches poor. Second, they mostly use the pixel-based fusion approach to combine every element of EMD, which could result in some spatial artifacts brought about by the pixel wise maps' noisy properties. Furthermore, these methods provide hazy fusion results since the fusion rules are unable to effectively capture the salient information of the input source images.

In this paper, we present a unique and fast EMD-based image fusion approach to enhance the performance of EMD-based image fusion methods. In order to break down the input source images into many IMFs with varying scales and a residue, we first create a multi-channel bidimensional EMD approach based on morphological filters (which we call MF-MBEMD). This method may greatly speed up the computation of EMD for multi-channel images. Then, to fuse the IMFs and residue, we employ a patch-based fusion technique with overlapping partition rather than the pixel-based fusion method often employed in EMD-based image fusion, where the energy-based rules are intended to extract the salient information of input source images. Lastly, we mix the fused residue and the fused IMFs together to achieve the final result.

## 2. RELATED WORK

### 2.1 Bi-dimensional empirical mode decomposition

In order to extract IMFs with varying scales, the original 1D EMD [3] used a sifting operation that required cubic splines to produce the upper and lower envelopes of every local extrema point (maxima and minima). Nunes et al. [12] created envelope surfaces using radial basis function interpolation in order to generalize it to 2D pictures. In order to increase the stability of BEMD, Al-Baddai et al. [13] presented a novel technique for envelope surface interpolation based on Green's function. The technique that computes the upper and lower envelopes [14–16] via bi-Laplacian operator interpolation was created to carry out the decomposition for signals defined on 3D surfaces, and it may be naturally adapted to 2D images [17, 18]. Pan and Yang [8] generated the mean surface by interpolating the centroid points of neighbor extremum points in their Delaunay triangulation in order to avoid computing the envelope surfaces during the sifting processing. In contrast, Qin et al. [6] computed the mean surface using a window function as an alternative, resulting in a window BEMD method. In order to optimize the decomposition by averaging the modes of all noise-added images, Wang et al. [9] introduced the bi-dimensional ensemble empirical mode decomposition method (BEEMD), which requires extremely high time costs. A direct envelope estimation method based on order-statistics filters [19] is proposed to generate the envelope surfaces of an input image, where the distance map between the adjacent maxima/minima is computed to determine the filter size. This approach aims to improve the computation efficiency of the surface interpolation-based BEMD methods. In order to further speed up the computation of envelope surfaces, Trusiak et al. created an improved rapid empirical mode decomposition approach [20] that uses morphological operations rather than order-statistics filters. Additionally, it can bypass the laborious computation of the distance map between the nearby extrema and creates the filter size just based on the extremum number.

The previously stated BEMD techniques are intended to break down 2D images that have a single data channel, or single-channel images. Even though they may also be used independently to break down each channel of a bivariate or multivariate 2D signal (two or more data channel), as [21] shows, they have a number of issues, including mode alignment and nonuniqueness. These problems restrict the use of EMD in data fusion, which calls for same-index IMFs with identically scaled data. Yeh [5] proposed the complex BEMD to decompose a bivariate (complex) 2D signal, which applies the standard BEMD based on surface interpolation [12] to four real-valued 2D signals to generate the complex-valued IMFs. This ensures that the extracted modes from each of the multiple 2D signals match in feature scales. To produce the multi-scale decomposition, Rehman et al. [7] reshaped a multi-channel 2D image into a multivariate 1D signal and applied the 1D multivariate EMD [22]. By estimating the mean surface of a multi-channel 2D image using n-dimensional surface projections, Xia et al. [10] improved this type of decomposition and were able to preserve its spatial information. In order to create the upper and lower envelopes of color images, Bhuiyan et al. [23] employed a direct envelope estimating approach based on order-statistics filters [19]. This method requires less time to complete than surface interpolation-based BEMD methods for multi-channel images. Inspired by the enhanced rapid empirical mode decomposition [20] developed for single-channel pictures, we use the morphological filters in this study to get the envelope surfaces of a multi-channel image in order to further reduce the decomposition time. It can greatly speed up the computation in addition to producing good decomposition results.

## 2.2 Image fusion

Numerous image fusion techniques, including transform domain, spatial domain, deep learning, and others, have been proposed as a result of advancements in signal processing and analysis. The transform domain techniques, which are more pertinent to EMD-based picture fusion, are the main topic of discussion here. A more thorough survey is available in [2,24, 25]. The fused image is produced by a reconstruction step using the corresponding inverse transform, and the transformed coefficients of the input source images acquired by a transform are combined using the transform domain methods. Without a doubt, one of the key components of these techniques is the transform domain selection. Numerous transforms, such as the Laplacian pyramid [26], multi-scale geometric analysis [27–30], fast Fourier transform [31], wavelet transform [32, 33], empirical mode decomposition (EMD) [4,5,7, 10], etc., have been used thus far to conduct image fusion. EMD is completely adaptive and data-driven, in contrast to many other classical transforms like the Fourier transform and wavelet transform, which use fixed basis functions. After breaking down the source images using the mean approximation-based BEMD, Pan and Yang [8] fused each component pixel by pixel using a standard deviation-based weighted averaging algorithm. A pixel-based image fusion technique based on BEEMD and an entropy-based weighted averaging rule were presented by Wang et al. [9] to carry out the fusion. Qin et al. [6] fused all IMFs and the residue using the maximum selection rule based on two saliency measures in a pixel-based way, which may create some artifacts. They obtained the decomposition using the window BEMD. The multivariate 1D EMD [22] are used to deconstruct source images in order to make the decompositions of various source images equal in quantity and property. Each component can then be blended pixel by pixel by a variance-based weighted averaging technique [7]. The multi-scale decomposition obtained by Xia et al. [10] using the multivariate BEMD based on surface projection can enhance the fusion quality of the multivariate 1D EMD-based fusion approach [7]. Yeh [5] suggested a multi-focus image fusion method based on pixels, taking into account the intricate BEMD. The raw images were broken down using the order-statistics filter-based EMD [19,23] by Ahmed and Manic [4]. A variance-based maximum selection method was then applied pixel by pixel to complete the fusion. Bivariate BEMD and sparse representation were used by Zhu et al. [11] to perform the fusion of infrared-visible images. The computational efficiency of the fusion schemes and the employed EMD methods limits the number of attempts that have been made in the investigation of EMD-based image fusion.

In this paper, we propose a novel and fast EMD-based image fusion method based on a patch and energy-based fusion strategy and a fast multi-channel bi-dimensional EMD method. Our method outperforms the existing EMD-based image fusion approaches on several widely used image data sets that contain multi-focus and multi-modal images.

## 2.3 Multi-channel bidimensional EMD based on morphological filter

The proposed MF-MBEMD employs the morphological filters with the same widow size for each channel to generate the envelope surfaces of a multi-channel image, which can extract similar spatial scale of each channel image during the decomposition. Specifically, given a multi-channel image  $I = (I_1, I_2, \dots, I_n)$  with the size  $W \times H$ , its upper envelope  $U = (U_1, U_2, \dots, U_n)$  and lower envelope  $D = (D_1, D_2, \dots, D_n)$  can be generated using equations (1) and (2) respectively.

$$U_K(x, y)|_{K=1,2,\dots,n} = (I_K \oplus b)(x, y) \quad (1)$$

$$D_K(x, y)|_{K=1,2,\dots,n} = (I_K \ominus b)(x, y) \quad (2)$$

Where  $\oplus$  denotes morphological expansion filter and  $\ominus$  denotes morphological corrosion filter. The average filter is used to get the smoothed envelopes as described in equations (3) and (4).

$$U'_K(x, y)|_{K=1,2,\dots,n} = \frac{1}{w \times w} \sum_{(s,t) \in Z_{xy}} U_K(s, t) \quad (3)$$

$$D'_K(x, y)|_{K=1,2,\dots,n} = \frac{1}{w \times w} \sum_{(s,t) \in Z_{xy}} D_K(s, t) \quad (4)$$

Here  $Z_{xy}$  represents the set of pixels in the window  $w \times w$  centered on the pixel  $(x, y)$  and  $b$  indicates the structuring element used during expansion and corrosion operations. To consider the feature extraction of all data channels of the input image, we set the window size  $w$  in Eq. (1), (2) and Eq. (3),(4) into the following minimal average extremum distance of all image channels.

$$w = \min (w_1, w_2, \dots, w_n) \quad (5)$$

$$w_k = \sqrt{\frac{W \times H}{N_k}} \tag{6}$$

where  $w_k$  ( $k = 1, \dots, n$ ) denotes the average extremum distance of the  $k$ -th channel image  $I_k$  and  $N_k$  is the average value of the numbers of all local maxima and minima of  $I_k$ . We find all local maxima (minima) of  $I_k$  by comparing the values of each pixel and its neighbours in the  $3 \times 3$  window centered on it in each iteration. It is different from the extraction of local extrema in the enhanced fast empirical mode decomposition method [20], where the size of extremum window is equal to the average extremum distance of the previous iteration and the number of extracted extrema is reduced. In contrast, this strategy obtains more extrema in each iteration and can extract much finer feature scale of each channel image. The proposed MF-MBEMD can extract the IMFs with different scales iteratively by a sifting processing based on the above envelope computation method until the specified number of IMFs is achieved or the residue is a constant or a monotonic function. Figures 1 and 2 give the decomposition results of some multi-focus images using MF-MBEMD. As can be seen that the leading IMFs extract much finer-scale features and the trailing IMFs describe much coarser-scale features. Furthermore, the extracted feature scales of two multi-focus images are matched very well for the same-index IMFs, which is very important for the application of EMD in image fusion.

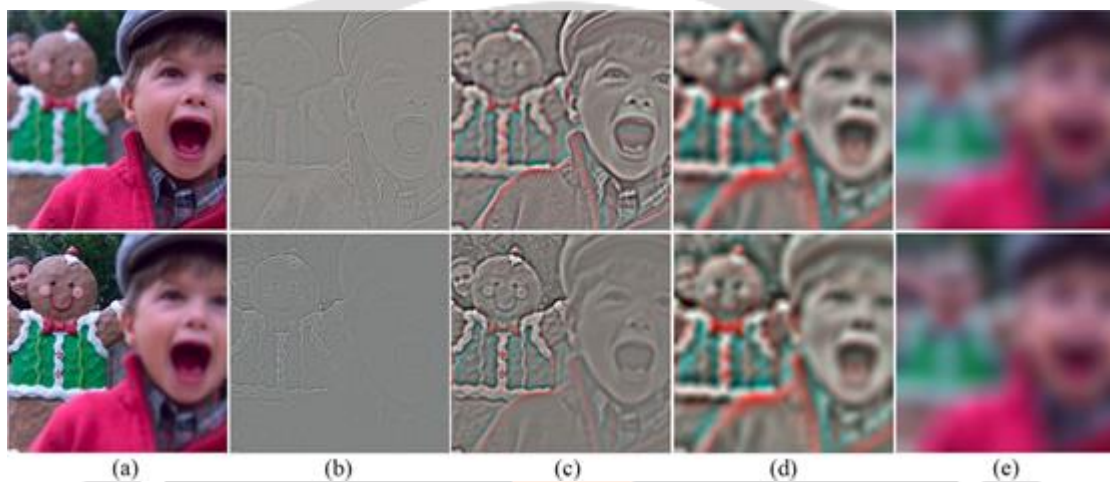


**Fig. 1. Decompositions of two color multi-focus images using MF-MBEMD**  
 Source images (b) IMF 1 (c) IMF 2 (d) IMF 3 (e) Residue

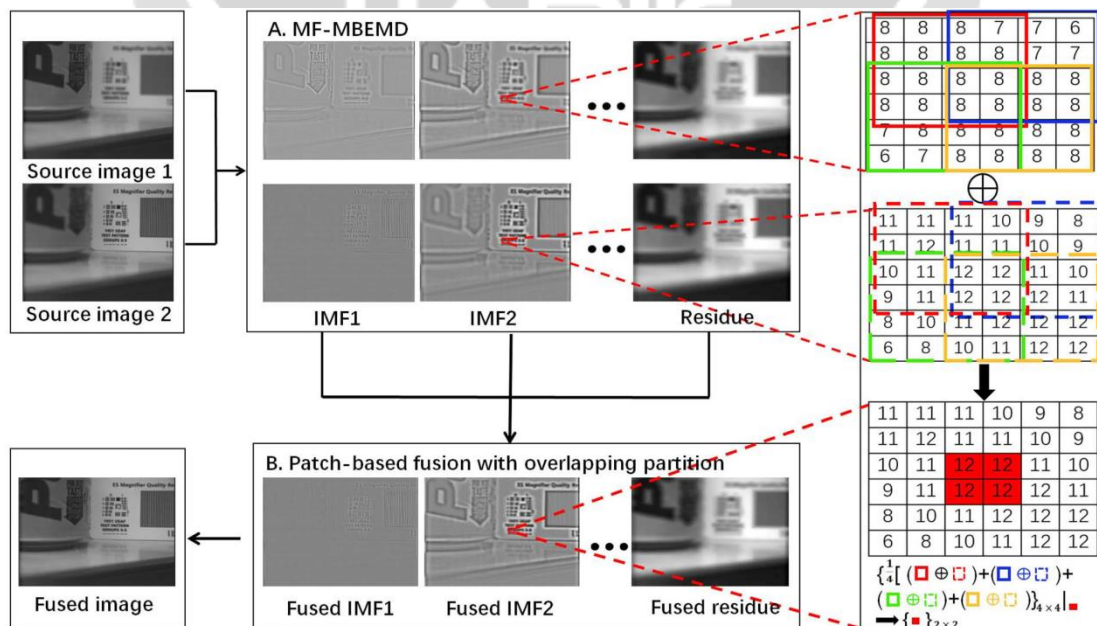


**Fig. 2. Image fusion using EMD**

### 3. PROPOSED METHODOLOGY

In the existing method of image fusion, after decomposing the images into IMFs and Residue, the IMFs and residues of both source images are combined using energy based fusion rule. In the proposed method, Image statistics are used to generate the weights of IMFs and IMFs are fused using these weights using weighted average fusion rule, while residues are fused using the energy based fusion rule as like existing method. The flow diagram of proposed method of image fusion is shown in figure 3.

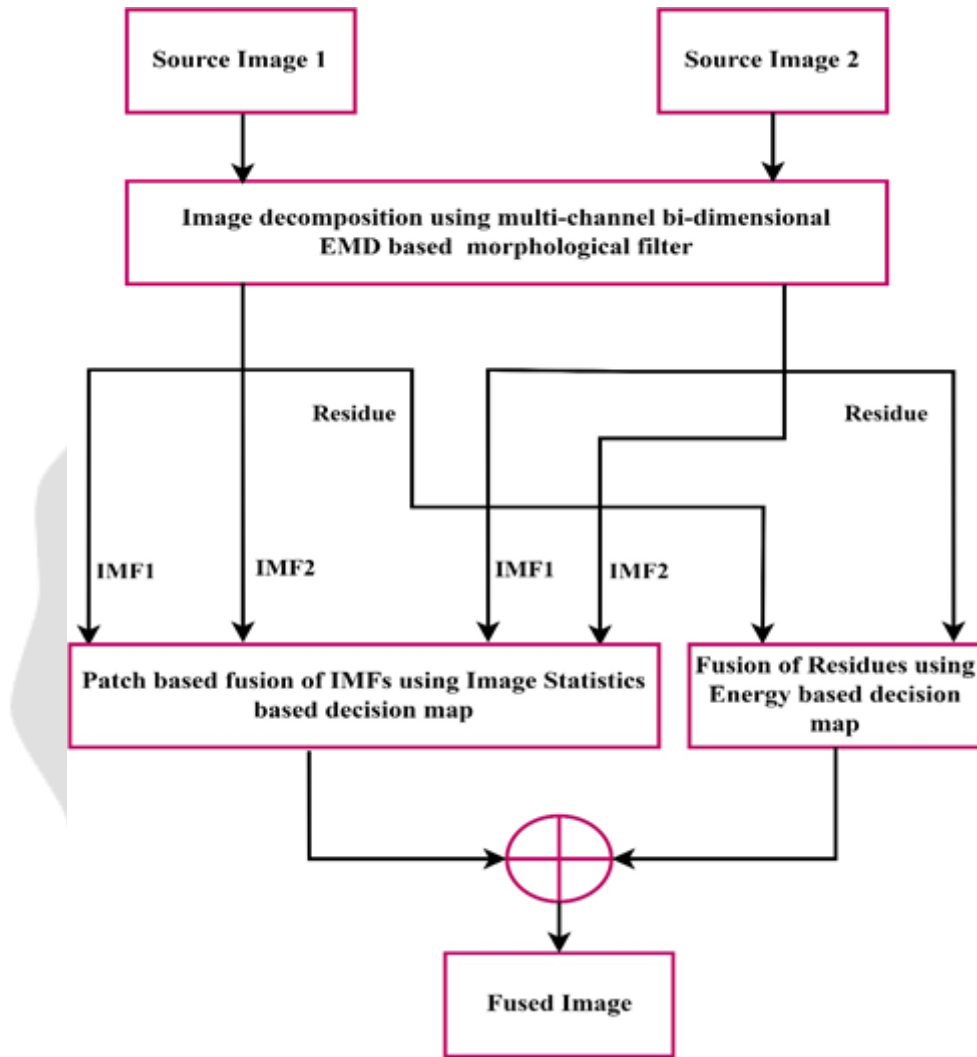


**Fig. 3. Flow diagram of proposed method**

Given two source images  $I_1$  and  $I_2$ , this method combines them into a two-channel image  $I = (I_1, I_2)$ , which can be decomposed into  $K$  IMFs with the scale from fine to coarse and a residue by MF-MBEMD as follows:

$$I = \sum_{i=1}^K F_i + R_K \tag{7}$$

Where  $F_i$  is the  $i$ th IMF and  $R_K$  is the  $K$ th residue.

For fusing the residues, as for the  $j$ -th patch  $R_K^j = (R_{K1}^j, R_{K2}^j)$  of the  $k$ -th residue  $R_K$  two different fusion rules based on the feature information extracted by IMFs to obtain the fusion residue patch  $H_K^j$  according to the image types are designed.

$$\begin{aligned}
 H_K^j &= R_{K1}^j & \text{if } E(R_{K1}^j) \geq E(R_{K2}^j) \\
 &R_{K2}^j & \text{if } E(R_{K1}^j) < E(R_{K2}^j)
 \end{aligned} \tag{8}$$

For fusing the IMFs, image statistics are used as follows: To determine the optimum weight, a square window of size  $n \times n$  is considered as a neighbourhood around detail coefficients  $F_i^j$  for each patch level  $j$  and is denoted by a matrix  $X$ . Determine the covariance matrix of  $X$  using equation (9) and unbiased estimate of  $X$ ,  $C_H^{u,v}(X)$  using equation (10) at pixel location  $(u, v)$  by treating the row as an observation and the column as a variable.

$$\text{Covariance}(X) = E[(X - E[X])(X - E[X])^T] \tag{9}$$

$$C_H^{u,v}(X) = \frac{1}{n-1} \sum_{z=1}^n (X_z - \bar{X})(X_z - \bar{X})^T \tag{10}$$

The variance vector is given by the diagonal elements of  $C_H^{u,v}(X)$ . Find the Eigen values of  $C_H^{u,v}(X)$ , which are given by  $\lambda_H$ . The sum of these Eigen values yields horizontal strength of detail layer  $F_i^j$ , which is given by equation (11).

$$\beta_H(u, v) = \sum_{j=1}^n \lambda_H^j \tag{11}$$

Using the same procedure, vertical estimate  $C_V^{u,v}(X)$  is obtained at pixel location  $(u, v)$  by treating the column as an observation and the row as a variable. Now find the Eigen values of  $C_V^{u,v}(X)$  and are given by  $\lambda_V$ . The sum of these Eigen values gives vertical strength of detail layer  $F_i^j$  and is given by equation (12).

$$\beta_V(u, v) = \sum_{j=1}^n \lambda_V^j \tag{12}$$

From  $\beta_H(u, v)$  and  $\beta_V(u, v)$ , the optimal weight of pixel located at  $(u, v)$  in the detail layer  $F_i^j$  is obtained using the equation (13).

$$W(u, v) = \beta_H(u, v) + \beta_V(u, v) \tag{13}$$

Using the above strategy, the weights are calculated for IMF components of source images  $I_1$  and  $I_2$ , which are given as  $W_1(u, v)$  and  $W_2(u, v)$ . By using the weights, the fused IMFs are calculated as follows:

$$G_i^j = \frac{(W_1^j(u, v) * F_{i1}^j + W_2^j(u, v) * F_{i2}^j)}{(W_1^j(u, v) + W_2^j(u, v))} \tag{14}$$

Once all patches of the IMFs and residue are fused, the value at each pixel  $(x, y)$  of the fused IMFs and residue are found by averaging the values of the pixel  $(x, y)$  in all overlapping patches by the following equations:

$$G_i^j(x, y) = \frac{1}{S(x, y)} \sum_j G_i^j(x, y) \tag{15}$$

$$H_k^j(x, y) = \frac{1}{S(x, y)} \sum_j H_k^j(x, y) \tag{16}$$

where  $S(x, y)$  denotes the overlapping patch number at the pixel  $(x, y)$ , and then the fused IMFs and the fused residue are added together to obtain the final fused image  $I'$

$$I'(x, y) = \sum_{i=1}^K G_i^j(x, y) + H_k^j(x, y) \tag{17}$$

#### 4. RESULTS AND DISCUSSION

In order to test the efficacy of proposed method in retaining precise details in the fused from the sources images, the proposed method is applied on multimodal image data sets pertaining to medical images, Multifocus image datasets and visible-IR image datasets. Further the performance of the proposed method is measured quantitatively using ten image quality assessment metrics like normalized mutual information ( $Q_{MI}$ ), Nonlinear correlation information entropy ( $Q_{NCIE}$ ), Phase congruency based metric ( $Q_P$ ), Structural similarity based metric ( $Q_E$ ), Edge Based Metric ( $Q_G$ ), Human perception inspired metric ( $Q_{CB}$ ) and ( $Q_{CV}$ ), Feature mutual information ( $Q_{FMI}$ ), Structural similarity based metric ( $Q_Y$ ) and visual information fidelity (QV IF). A qualitative and quantitative comparison is made between existing and proposed methods, which are presented in this chapter. All the source images are collected from the publicly available benchmark datasets at <https://github.com/yuliu316316/MFIF>.

## 4.1 Performance metrics

### 1. Normalized Mutual Information ( $Q_{MI}$ )

$$Q_{MI} = 2 \left[ \frac{MI(A,F)}{H(A)+H(F)} + \frac{MI(B,F)}{H(B)+H(F)} \right] \quad (18)$$

Where  $H(A)$ ,  $H(B)$ ,  $H(F)$  represents entropy of input images A,B and fused image F respectively.

$MI(A, F)$ - Mutual Information between A and F

$MI(B, F)$ - Mutual Information between B and F

It measures the mutual dependence of two variables and evaluate the intensity similarity of the fused image.

### 2. Nonlinear correlation information entropy ( $Q_{NCIE}$ )

$$Q_{NCIE} = 1 + \sum_{i=1}^3 \frac{\lambda_i}{3} \log_{256} \frac{\lambda_i}{3} \quad (19)$$

Where  $\lambda_i$  are the Eigen values of Non linear correlation matrix. It measures the nonlinear correlation information entropy.

### 3. Phase congruency based metric ( $Q_P$ )

$$Q_P = (P_p)^\alpha (P_M)^\beta (P_m)^\gamma \quad (20)$$

$P_p$ ,  $P_M$  and  $P_m$  are all calculated as the maximum correlation coefficients between the fused image and the source images.  $p$ ,  $M$  and  $m$  represents phase congruency, maximum and minimum moments. The exponential parameters  $\alpha$ ,  $\beta$  and  $\gamma$  are used to adjust the significance of the three components.

### 4. Structural similarity based metric ( $Q_E$ )

$$Q_E = \frac{(2\mu_A\mu_F+C1)(2\sigma_{AF}+C2)}{(\mu_A^2+\mu_F^2+C1)(\sigma_A^2+\sigma_F^2+C2)} \quad (21)$$

Where  $\mu_A$  is the mean of source image A and  $\mu_F$  is the mean of fused image F,  $\sigma_{AF}$  is the co-variance of A and F,  $\sigma_A^2$  is the variance of A and  $\sigma_F^2$  is the variance of F, C1 and C2 are constants.

### 5. Edge Based Metric ( $Q_G$ )

$$Q_G = \sum_{i=1}^H \sum_{j=1}^W \left[ \frac{Q^{AF}(i,j)w^A(i,j) + Q^{BF}(i,j)w^B(i,j)}{w^A(i,j) + w^B(i,j)} \right] \quad (22)$$

Where H,W are row and column dimensions of an image

$Q^{AF}(i, j)$  – edge strength between A and F at pixel (i,j)

$Q^{BF}(i, j)$  – edge strength between A and F at pixel (i,j)

$w^A(i, j)$ ,  $w^B(i, j)$ - Weighting factors

It evaluate the gradient information retained by the fused image.

### 6. Human perception inspired metric ( $Q_{CB}$ )

$$Q_{CB} = \lambda_A(i, j)Q_{AF}(i, j) + \lambda_B(i, j)Q_{BF}(i, j) \quad (23)$$

$Q_{AF}$ ,  $Q_{BF}$  –contrast information between source images and fused image F.

$\lambda_A$ ,  $\lambda_B$ - Saliency maps of source images.

$$Q_{CV} = \frac{\sum_{l=1}^L (\lambda(I_A^{W1})D(I_A^{W1}, I_F^{W1}) + \lambda(I_B^{W1})D(I_B^{W1}, I_F^{W1}))}{\sum_{l=1}^L (\lambda(I_A^{W1}) + \lambda(I_B^{W1}))} \quad (24)$$

$D(I_A^{W1}, I_F^{W1})$ ,  $D(I_B^{W1}, I_F^{W1})$  are the local similarity values between source images and fused image.

They evaluate the local significance and contrast information retained by the fused image.

**7. Feature mutual information ( $Q_{FMI}$ )**

$$Q_{FMI} = \frac{MI(A,F)}{H(A)+H(F)} + \frac{MI(B,F)}{H(B)+H(F)} \tag{25}$$

**8. Structural similarity based metric ( $Q_Y$ )**

$$Q_Y = \lambda(w)Q_E(A, F) + (1 - \lambda(w))Q_E(B, F) \quad \text{if } Q_E(A, B) \geq 0.75 \tag{26}$$

$$\text{Max}(Q_E(A, F), Q_E(B, F)) \quad \text{if } Q_E(A, B) < 0.75$$

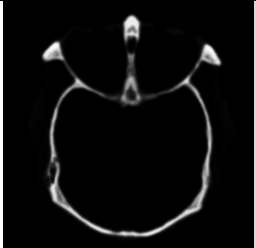
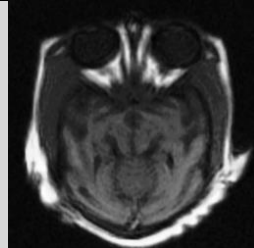
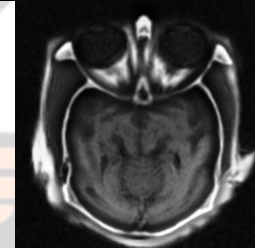
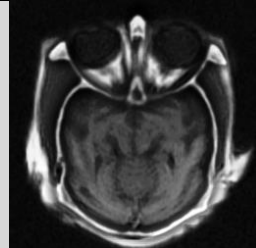
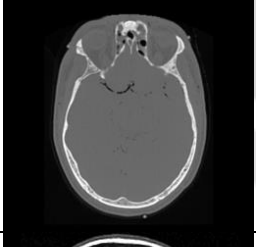
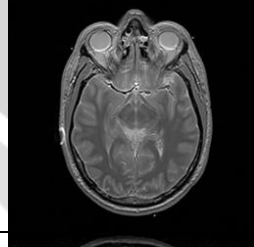
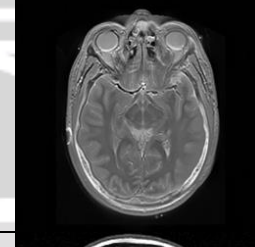
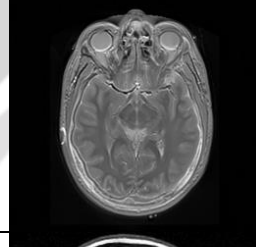
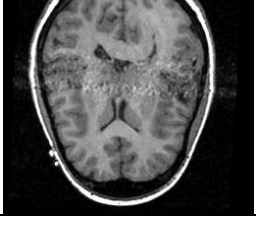
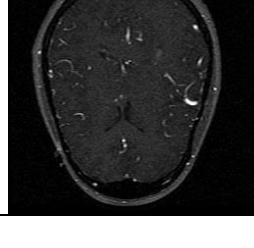
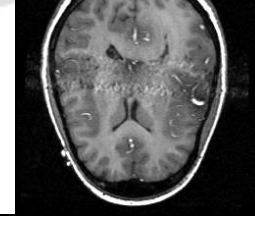
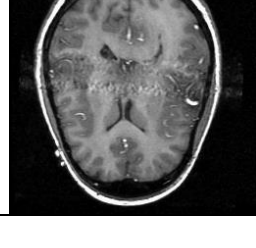
It evaluates the fused image from brightness, contrast, and structure.

**9. Visual Fidelity Information ( $Q_{VIF}$ ) :** It measures the fidelity of the visual information of the fused image relative to the source images.

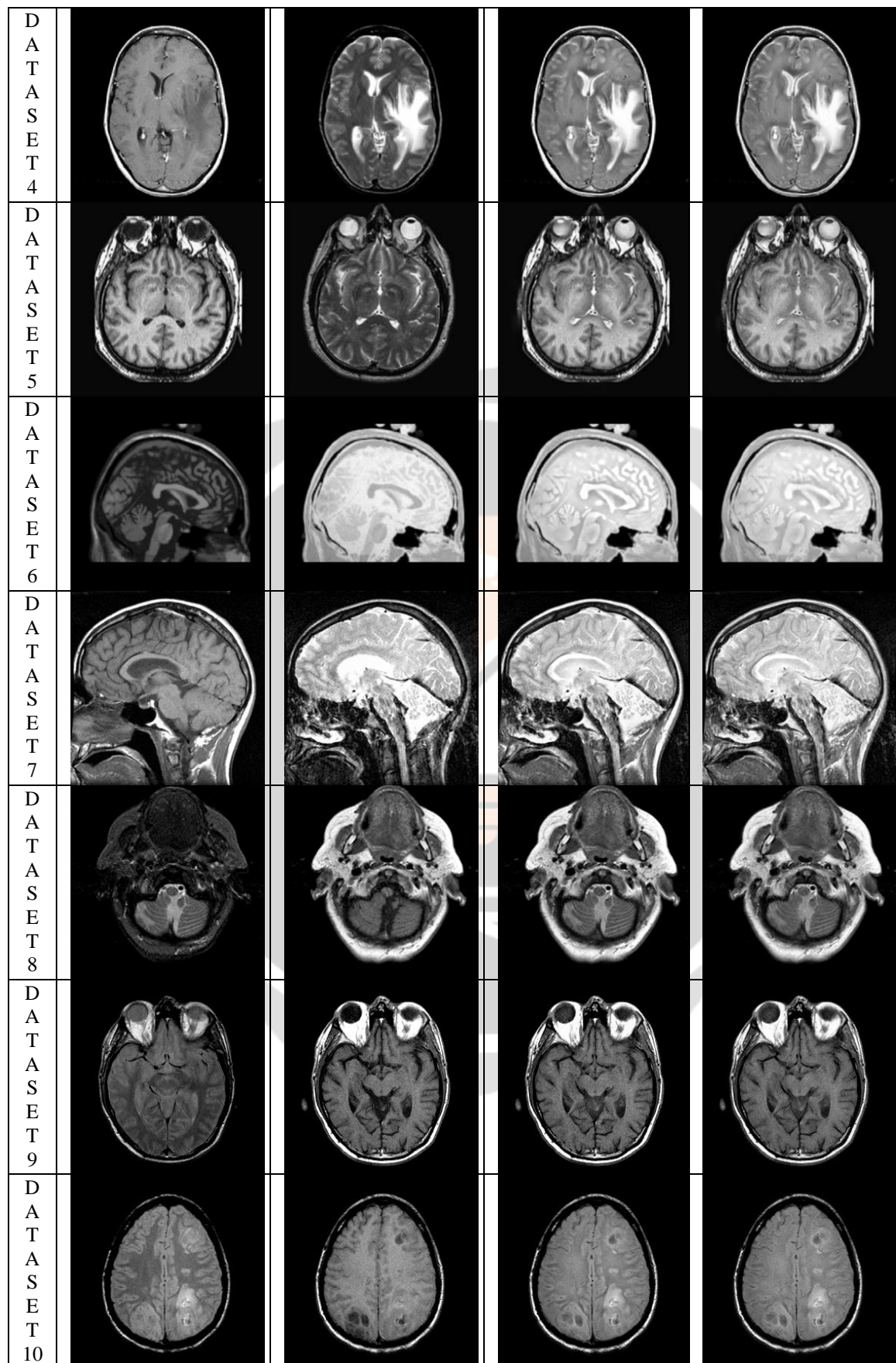
All the above metrics should be considered as better if they produce higher value except QCV, for which the value is smaller for the fused image.

**4.2 Fusion results of medical image data sets of brain**

In order to assess the performance of proposed method in image fusion, it is applied on sixteen medical image data sets related to various disorders of brain and the fusion results are presented in figure 4 for both existing and proposed methods. In the figure 4, (a) and (b) represents the source images considered for fusion, while (c) and (d) depicts the fused images produced using existing and proposed methods respectively.

	CT Scan Image	MRI Scan Image	Existing Method Fused Image	Proposed Method Fused Image
D A T A S E T 1				
D A T A S E T 2				
D A T A S E T 3				





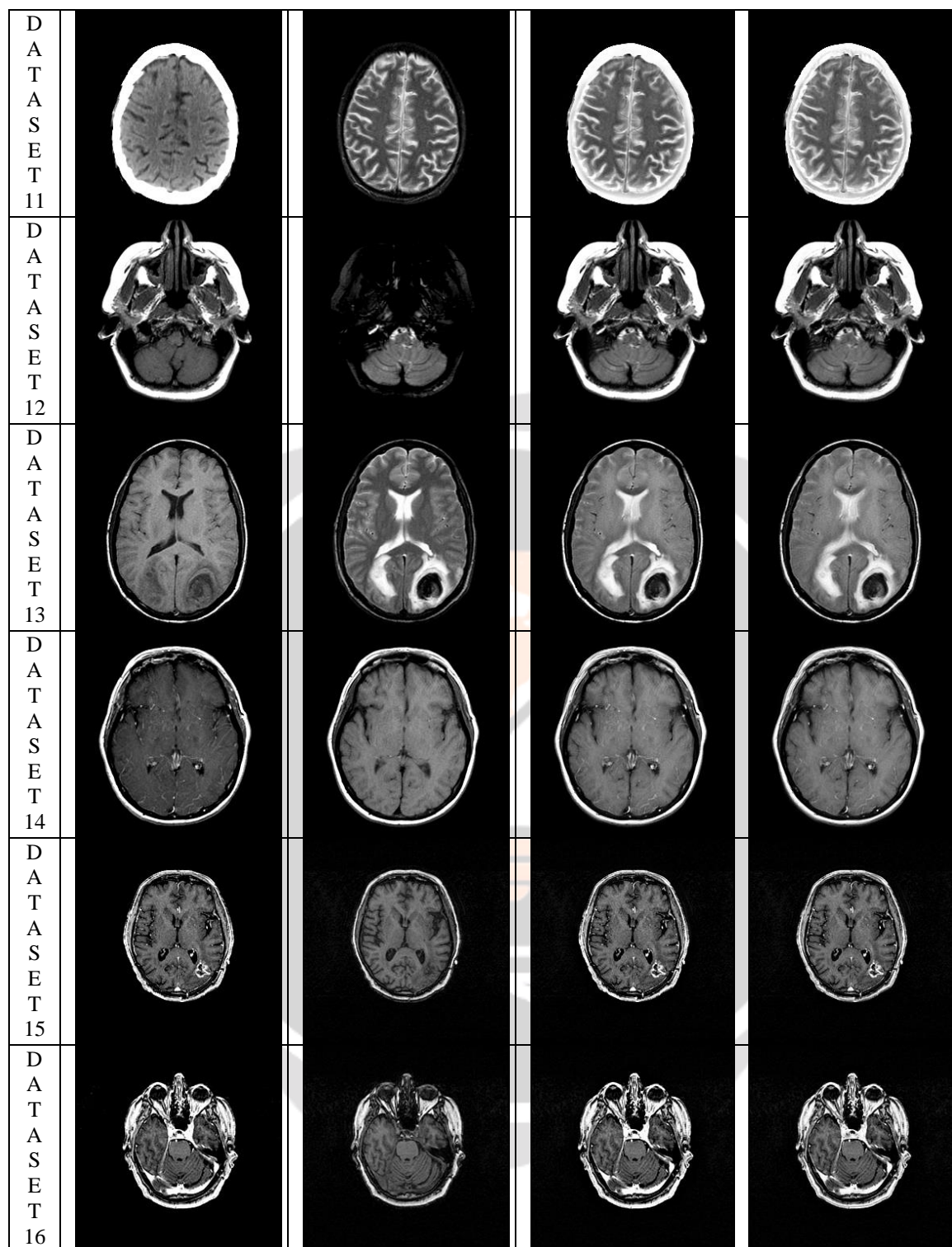


**Fig. 4. Fusion results of medical datasets**

The values of fused image quality measurement metrics for the above sixteen data sets are presented in table 1 for existing method and table 2 for the proposed method. From the quantitative results, it is revealed that the proposed method surpassed the existing method in every parameter for almost all medical images pertaining to various disorders of brain.

**Table 1. Performance metrics of Existing method**

Dataset Number	Q <sub>MI</sub>	Q <sub>FMI</sub>	Q <sub>NCIE</sub>	Q <sub>G</sub>	Q <sub>P</sub>	Q <sub>E</sub>	Q <sub>Y</sub>	Q <sub>CB</sub>	Q <sub>CV</sub>	Q <sub>VIF</sub>
1	0.693	0.906	0.814	0.743	0.570	0.667	0.888	0.351	1056.982	0.804
2	0.803	0.887	0.810	0.622	0.580	0.433	0.895	0.529	826.705	0.939
3	0.880	0.919	0.814	0.652	0.623	0.813	0.910	0.632	70.480	1.090
4	0.838	0.909	0.810	0.653	0.491	0.704	0.916	0.744	258.906	0.825
5	0.772	0.873	0.814	0.608	0.538	0.572	0.894	0.630	350.564	0.788
6	0.820	0.909	0.811	0.662	0.447	0.716	0.829	0.611	239.261	0.936
7	0.524	0.863	0.811	0.568	0.473	0.581	0.871	0.583	837.931	0.716
8	0.939	0.881	0.816	0.655	0.669	0.728	0.949	0.640	169.821	1.140
9	0.934	0.919	0.811	0.717	0.731	0.740	0.976	0.780	195.478	1.141
10	0.827	0.943	0.808	0.671	0.468	0.794	0.939	0.786	142.808	1.108
11	0.847	0.891	0.807	0.561	0.455	0.680	0.909	0.751	216.750	0.785
12	0.954	0.883	0.809	0.783	0.698	0.888	0.980	0.705	67.562	1.049
13	0.791	0.921	0.810	0.619	0.434	0.716	0.909	0.744	163.431	0.849
14	0.814	0.919	0.808	0.634	0.510	0.652	0.909	0.731	712.993	1.056
15	1.033	0.934	0.810	0.720	0.893	0.701	0.957	0.570	435.078	1.619
16	1.011	0.919	0.812	0.721	0.845	0.736	0.957	0.556	395.075	1.533

**Table 2. Performance metrics of Proposed method**

Dataset Number	Q <sub>MI</sub>	Q <sub>FMI</sub>	Q <sub>NCIE</sub>	Q <sub>G</sub>	Q <sub>P</sub>	Q <sub>E</sub>	Q <sub>Y</sub>	Q <sub>CB</sub>	Q <sub>CV</sub>	Q <sub>VIF</sub>
1	0.780	0.937	0.843	0.790	0.678	0.708	0.947	0.351	1103.078	0.867
2	0.897	0.898	0.840	0.631	0.610	0.443	0.938	0.512	769.438	0.975
3	0.889	0.943	0.842	0.657	0.650	0.842	0.911	0.596	81.388	1.085
4	0.872	0.930	0.839	0.664	0.496	0.720	0.917	0.713	300.790	0.842
5	0.799	0.892	0.842	0.590	0.489	0.583	0.904	0.578	368.675	0.782
6	0.843	0.935	0.840	0.659	0.475	0.742	0.827	0.592	239.697	0.948
7	0.574	0.879	0.839	0.581	0.499	0.599	0.874	0.518	783.305	0.669
8	0.847	0.892	0.840	0.617	0.621	0.736	0.942	0.602	172.559	1.097
9	0.874	0.935	0.838	0.722	0.709	0.784	0.958	0.733	193.776	1.113
10	0.871	0.971	0.837	0.683	0.476	0.835	0.940	0.749	127.171	1.116
11	0.909	0.915	0.836	0.570	0.455	0.708	0.925	0.728	271.711	0.803

<b>12</b>	0.907	0.910	0.837	0.800	0.731	0.918	0.996	0.692	76.811	1.072
<b>13</b>	0.842	0.946	0.839	0.615	0.422	0.730	0.910	0.716	181.839	0.888
<b>14</b>	0.896	0.943	0.838	0.663	0.539	0.703	0.915	0.717	630.065	1.085
<b>15</b>	1.099	0.954	0.840	0.746	0.914	0.756	1.009	0.564	355.447	1.634
<b>16</b>	1.031	0.934	0.842	0.738	0.860	0.781	0.999	0.541	359.856	1.487

The average values of sixteen data sets for the existing and proposed method are presented in table 3. From the table 3, it is revealed that the proposed method is effective in diagnosing the brain disorders when compared to existing method. Hence the proposed method is recommended to the physician to fuse the medical images so that they can identify the disorders more accurately and treat the patient with required medical care.

**Table 3. Average values of performance metrics for medical datasets**

Method	Q <sub>MI</sub>	Q <sub>FMI</sub>	Q <sub>NCIE</sub>	Q <sub>G</sub>	Q <sub>P</sub>	Q <sub>E</sub>	Q <sub>Y</sub>	Q <sub>CB</sub>	Q <sub>CV</sub>	Q <sub>VIF</sub>
<b>Existing</b>	0.842	0.905	0.811	0.662	0.589	0.695	0.918	0.647	383.739	1.024
<b>Proposed</b>	<b>0.871</b>	<b>0.926</b>	<b>0.840</b>	<b>0.670</b>	<b>0.601</b>	<b>0.724</b>	<b>0.932</b>	<b>0.619</b>	<b>375.975</b>	<b>1.029</b>

### 4.3 Fusion results of multi focus image data sets

In order to assess the performance of proposed method in image fusion, it is applied on ten multi-focus image data sets related to various scenes and the fusion results are presented in figure 5 for both existing and proposed methods. In the figure 5, (a) and (b) represents the left and right focus source images considered for fusion, while (c) and (d) depicts the fused images produced using existing and proposed methods respectively.

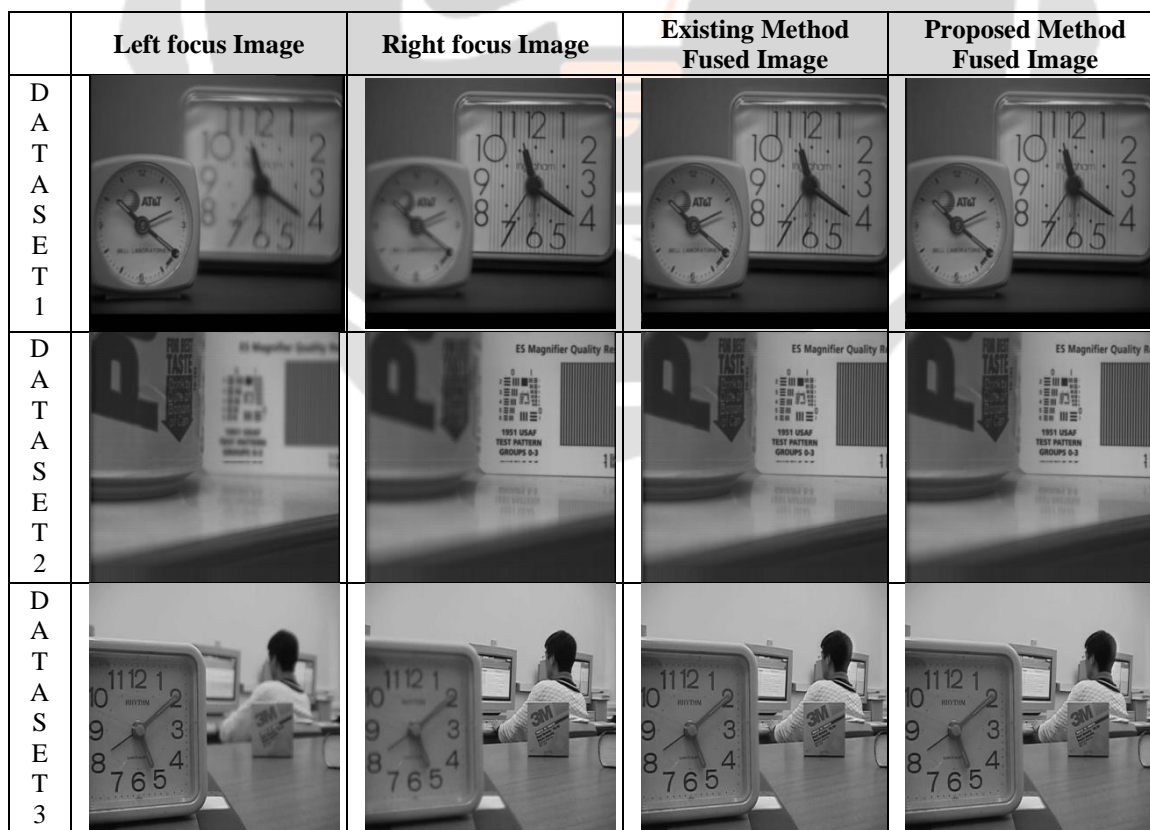




Fig. 5. Fusion results of multi-focus datasets

The values of fused image quality measurement metrics for the above ten data sets are presented in table 4 for existing method and table 5 for the proposed method. From the quantitative results, it is revealed that the proposed method surpassed the existing method in every parameter for all multi-focus images pertaining to various scenes.

**Table 4. Performance metrics of Existing method for multi-focus images**

Dataset Number	Q <sub>MI</sub>	Q <sub>FMI</sub>	Q <sub>NCIE</sub>	Q <sub>G</sub>	Q <sub>P</sub>	Q <sub>E</sub>	Q <sub>Y</sub>	Q <sub>CB</sub>	Q <sub>CV</sub>	Q <sub>VIF</sub>
1	1.019	0.923	0.831	0.703	0.798	0.822	0.942	0.703	45.560	1.551
2	0.999	0.924	0.830	0.778	0.861	0.903	0.958	0.659	26.168	1.544
3	1.062	0.919	0.832	0.732	0.782	0.862	0.945	0.683	9.606	1.512
4	0.876	0.911	0.824	0.721	0.791	0.861	0.948	0.710	34.561	1.385
5	0.986	0.890	0.827	0.713	0.774	0.834	0.971	0.764	49.803	1.579
6	0.861	0.847	0.824	0.704	0.889	0.800	0.946	0.752	72.903	1.490
7	0.961	0.902	0.830	0.705	0.884	0.851	0.973	0.730	56.726	1.460
8	0.815	0.874	0.822	0.702	0.751	0.826	0.971	0.792	29.043	1.659
9	0.496	0.770	0.809	0.662	0.635	0.648	0.984	0.721	85.699	1.063
10	1.184	0.938	0.835	0.722	0.772	0.811	0.939	0.710	8.717	1.592

**Table 5. Performance metrics of Proposed method for multi-focus images**

Dataset Number	Q <sub>MI</sub>	Q <sub>FMI</sub>	Q <sub>NCIE</sub>	Q <sub>G</sub>	Q <sub>P</sub>	Q <sub>E</sub>	Q <sub>Y</sub>	Q <sub>CB</sub>	Q <sub>CV</sub>	Q <sub>VIF</sub>
1	1.101	0.952	0.860	0.724	0.861	0.855	0.956	0.695	45.788	1.619
2	1.094	0.953	0.860	0.807	0.940	0.938	0.996	0.634	24.038	1.611
3	1.147	0.947	0.862	0.750	0.850	0.895	0.972	0.673	10.252	1.574
4	0.964	0.940	0.854	0.742	0.870	0.893	0.973	0.703	34.183	1.446
5	1.054	0.918	0.856	0.740	0.871	0.873	1.001	0.757	49.265	1.642
6	0.913	0.873	0.853	0.711	0.962	0.842	0.930	0.742	64.363	1.539
7	0.998	0.929	0.857	0.711	0.928	0.884	0.955	0.675	50.115	1.475
8	0.870	0.897	0.849	0.729	0.851	0.868	0.999	0.769	28.333	1.725
9	0.410	0.802	0.834	0.575	0.595	0.631	0.951	0.599	89.468	0.880
10	1.248	0.960	0.864	0.733	0.829	0.852	0.935	0.675	10.468	1.591

The average values of ten data sets for the existing and proposed method are presented in table 6. From the table 6, it is revealed that the proposed method is effective in fusing the multi-focus images when compared to existing method. Hence the proposed method is recommended for fusion of images related to multi-focus applications.

**Table 6. Average Values of performance metrics for multi-focus images**

Method	Q <sub>MI</sub>	Q <sub>FMI</sub>	Q <sub>NCIE</sub>	Q <sub>G</sub>	Q <sub>P</sub>	Q <sub>E</sub>	Q <sub>Y</sub>	Q <sub>CB</sub>	Q <sub>CV</sub>	Q <sub>VIF</sub>
Existing	0.926	0.890	0.826	0.714	0.794	0.822	0.958	0.722	41.879	1.483
Proposed	<b>0.980</b>	<b>0.917</b>	<b>0.855</b>	<b>0.722</b>	<b>0.856</b>	<b>0.853</b>	<b>0.967</b>	<b>0.692</b>	<b>40.627</b>	<b>1.510</b>

From the average values of performance metrics, the proposed method could improve the normalized mutual information in the fused image by 3.3 % for medical images, 5.5% for multi-focus images and 7.6% for infrared and visible images when compared to existing method as depicted in figure 6(a). The proposed method could improve the normalized feature mutual information in the fused image by 2.2 % for medical images, 2.9% for multi-focus images and 2.8% for infrared and visible images when compared to existing method as depicted in figure 6(b). The proposed method could improve the correlation information entropy in the fused image by 3.4 % for medical images, 3.3% for multi-focus images and 3.2% for infrared and visible images when compared to existing method as depicted in figure 6(c).

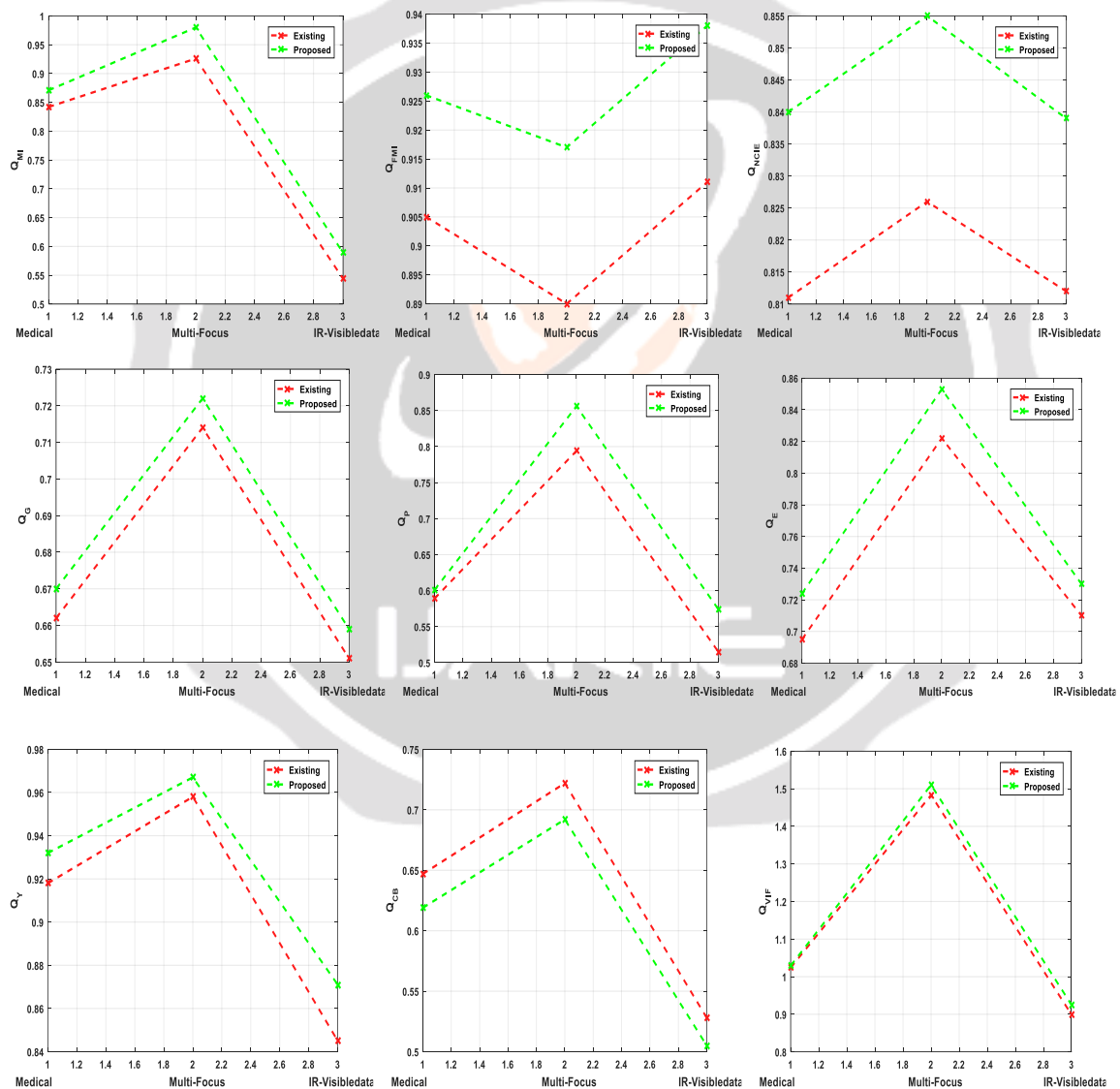


Fig. 6. Comparative analysis of visual fidelity information metric of various datasets

The proposed method could improve the edge information in the fused image by 1.3 % for medical images, 1.1% for multi-focus images and 1.2% for infrared and visible images when compared to existing method as depicted in figure 6(d). The proposed method could improve the phase congruent information in the fused image by 2 %

for medical images, 7.2% for multi-focus images and 10% for infrared and visible images when compared to existing method as depicted in figure 6(e). The proposed method could improve the structural information in the fused image by 4 % for medical images, 3.6% for multi-focus images and 2.7% for infrared and visible images when compared to existing method as depicted in figure 6(f). The proposed method could improve the structural similarity in the fused image by 1.5 % for medical images, 0.5% for multi-focus images and 2.9% for infrared and visible images when compared to existing method as depicted in figure 6(g). The proposed method could improve the visual perception of the fused image by 4.1 % for medical images, 4.2% for multi-focus images and 4.3% for infrared and visible images when compared to existing method as depicted in figure 6(h). The proposed method could improve the visual fidelity information in the fused image by 0.5 % for medical images, 1.7% for multi-focus images and 2.8% for infrared and visible images when compared to existing method as depicted in figure 6(i).

## 5. CONCLUSION

In this paper, we have presented a novel and fast EMD based image fusion method via morphological filter in order to generate high-quality fusion images. A multi-channel bi-dimensional EMD method based on morphological filter (MF-MBEMD) is first developed to decompose the input images into several IMFs with different scales and a residue, which uses the morphological expansion and erosion filters to compute the upper and lower envelopes of a multi-channel image. It can significantly improve the computation efficiency of EMD-based image fusion techniques. And then, a patch-based fusion strategy with overlapping partition is adopted to instead the pixel-based fusion method commonly used in EMD-based image fusion, where an image statistics based weighted average rule is designed to fuse the IMFs, and the feature information extracted by IMFs is used as a guide to merge the residue. Finally, the final result is generated by adding all fused IMFs and fused residue together. The performance evaluation of the EMD-based image fusion methods on several commonly used data sets with multi-focus and multi-modal images shows that our newly proposed image fusion method obtains better results. Furthermore, a large number of comparative experiments have also demonstrated our method is very competitive with the state-of-the-art image fusion methods in visualization, objective metrics, and time performance.

## REFERENCES

1. Goshtasby, A.A., Nikolov, S.: Image fusion: advances in the state of the art. *Inf. Fus.* 8(2), 114–118 (2007)
2. Ma, J., Ma, Y., Li, C.: Infrared and visible image fusion methods and applications: a survey, *Inf. Fus.* pp 153–178 (2019)
3. Huang, N.E., Shen, Z., Long, S.R., Wu, M.C., Shih, H.H., Zheng, Q., Yen, N.C., Tung, C.C., Liu, H.H.: The empirical mode decomposition and the hilbert spectrum for nonlinear and non-stationary time series analysis. *Proc. Math. Phys. Eng. Sci.* 454(1971), 903–995 (1998)
4. Ahmed, M.U., Mandic, D.P.: Image fusion based on fast and adaptive bidimensional empirical mode decomposition, In: 2010 13th International Conference on Information Fusion, 2010, pp. 1–6
5. Yeh, M.H.: The complex bidimensional empirical mode decomposition. *Signal Process.* 92(2), 523–541 (2012)
6. Qin, X., Zheng, J., Hu, G., Wang, J.: Multi-focus image fusion based on window empirical mode decomposition. *Infrared Phys. Technol.* 85, 251–260 (2017)
7. Rehman, N., Ehsan, S., Abdullah, S., Akhtar, M., Mandic, D., McDonald-Maier, K.: Multi-scale pixel-based image fusion using multivariate empirical mode decomposition. *Sensors* 15(5), 10923–10947 (2015)
8. Pan, J., Tang, Y.Y.: A mean approximation based bidimensional empirical mode decomposition with application to image fusion. *Digital Signal Process.* 50, 61–71 (2016)
9. Wang, P., Fu, H., Zhang, K.: A pixel-level entropy-weighted image fusion algorithm based on bidimensional ensemble empirical mode decomposition. *Int. J. Distrib. Sens. Netw.* 14(12), 1–16 (2018)
10. Xia, Y., Zhang, B., Pei, W., Mandic, D.P.: Bidimensional multivariate empirical mode decomposition with applications in multi-scale image fusion. *IEEE Access* 7, 114261–114270 (2019)
11. Zhu, P., Liu, L., Zhou, X.: Infrared polarization and intensity image fusion based on bivariate bemd and sparse representation. *Multimed. Tools Appl.* 80, 4455–4471 (2021)
12. Nunes, J.C., Bouaoune, Y., Delechelle, E., Niang, O., Bunel, P.: Image analysis by bidimensional empirical mode decomposition. *Image Vis. Comput.* 21(12), 1019–1026 (2003)
13. Al-Baddai, S., Al-Subari, K., Tom, A.M., Sol-Casals, J., Lang, E.W.: A green function-based bi-dimensional empirical mode decomposition. *Inf. Sci.* 348, 305–321 (2016)



14. Hu, J., Wang, X., Qin, H.: Improved, feature-centric emd for 3d surface modeling and processing. *Graph. Models* 76(5), 340–354 (2014)
15. Hu, J., Wang, X., Qin, H.: Novel and efficient computation of hilbert-huang transform on surfaces. *Comput.Aided Geom.Design* 43, 95–108 (2016)
16. Wang, X., Hu, J., Guo, L., Zhang, D., Hong, Q., Hao, A.: Featurepreserving, mesh-free empirical mode decomposition for point clouds and its applications. *Comput. Aided Geomet. Design* 59, 1–16 (2018)
17. Wang, X., Hu, K., Hu, J., Du, L., Ho, A.T.S., Qin, H.: Robust and blind image watermarking via circular embedding and bidimensional empirical mode decomposition. *Vis. Comput.* 36(19), 2201–2214 (2020)
18. Wang, X., Hu, K., Hu, J., Du, L., Ho, A.T.S., Qin, H.: A novel robust zero-watermarking algorithm for medical images. *Vis. Comput.* 37, 2841–2853 (2021)
19. Bhuiyan, S., Adhami, R.R., Khan, J.F.: Fast and adaptive bidimensional empirical mode decomposition using order-statistics filter based envelope estimation. *Eurasip J. Adv. Signal Process.* 2008(164), 1–18 (2008)
20. Trusiak, M., Wielgus, M., Patorski, K.: Advanced processing of optical fringe patterns by automated selective reconstruction and enhanced fast empirical mode decomposition. *Opt. Lasers Eng.* 52, 230–240 (2014)
21. Mandic, D.P., urRehman, N., Wu, Z., Huang, N.E.: Empirical mode decomposition-based time-frequency analysis of multivariate signals: the power of adaptive data analysis. *IEEE Signal Process. Mag.* 30(6), 74–86 (2013)
22. Rehman, N., Mandic, D.P.: Multivariate empirical mode decomposition. *Proc.R. Soc.A Math. Phys. Eng. Sci.* 466(2117), 1291–1302 (2010)
23. Bhuiyan, S., Khan, J.F., Alam, M.S., Adhami, R.R.: Color image trend adjustment using a color bidimensional empirical mode decomposition method. *J. Electron. Imaging* 21(3), 234–242 (2012)
24. Liu, Y., Chen, X., Wang, Z., Wang, Z.J., Ward, R.K., Wang, X.: Deep learning for pixel-level image fusion: recent advances and future prospects. *Inf. Fus.* 42, 158–173 (2018)
25. Yu, L., Lei, W., Juan, C., Chang, L., Xun, C.: Multi-focus image fusion: a survey of the state of the art. *Inf. Fus.* 64, 71–91 (2020)
26. Sufyan, A., Imran, M., Shah, S.A., Shahwani, H., Wadood, A.A.: A novel multimodality anatomical image fusion method based on contrast and structure extraction. *Int. J. Imag. Syst. Technol.* 32(1), 324–342 (2022)
27. Li, X., Li, H., Yu, Z., Kong, Y.: Multifocus image fusion scheme based on the multiscale curvature in nonsubsampling contourlet transform domain. *Opt. Eng.* 54(7), 1–15 (2015)
28. Li, H., Chai, Y., Li, Z.: Multi-focus image fusion based on nonsubsampling contourlet transform and focused regions detection. *Optik Int. J. Light Electron Opt.* 124(1), 40–51 (2013)
29. Nencini, F., Garzelli, A., Baronti, S., Alparone, L.: Remote sensing image fusion using the curvelet transform. *Inf. Fus.* 8(2), 143–156 (2007)
30. Liu, Y., Liu, S., Wang, Z.: A general framework for image fusion based on multi-scale transform and sparse representation. *Inf. Fus.* 24, 147–164 (2015)
31. Naidu, V.: Multi-resolution image fusion by fft, In: *International Conference on Image Information Processing 2011*, 1–6 (2011)
32. Li, H., Manjunath, B.S., Mitra, S.: Multisensor image fusion using the wavelet transform. *Gr. Models Image Process.* 57(3), 235–245 (1995)
33. Lewis, J.J., OCallaghan, R., Nikolov, S.G., Bull, D.R., Canagarajah, N.: Pixel- and region-based image fusion with complex wavelets. *Inf. Fus.* 8(2), 119–130 (2007)
34. Yu, Z.A., Yu, L.B., Peng, S.C., Han, Y.A., Xz, D., Li, Z.A.: Ifcnn: a general image fusion framework based on convolutional neural network. *Inf. Fus.* 54, 99–118 (2020)
35. Haghghat, M.B.A., Aghagolzadeh, A., Seyedarabi, H.: A nonreference image fusion metric based on mutual information of image features. *Comput. Electr. Eng.* 37(5), 744–756 (2011).